

Combination of On-Chip Field Amplification and Bovine Serum Albumin Sweeping for Ultrasensitive Detection of Green Fluorescent Protein

Qiong Pan and Meiping Zhao*

Beijing National Laboratory for Molecular Sciences, Key Laboratory of Bioorganic Chemistry & Molecular Engineering of Ministry of Education, College of Chemistry and Molecular Engineering, Peking University, Beijing, 100871, People's Republic of China

Shaorong Liu*

Department of Chemistry and Biochemistry, The University of Oklahoma, Norman, Oklahoma 73019

We report a highly effective on-chip preconcentration method by combining field-amplified sample injection (FASI) and bovine serum albumin (BSA) sweeping for ultrasensitive detection of green fluorescent protein (GFP) on a simple cross-channel microchip device. With the formation of a stagnant sample/running buffer boundary by balancing the hydrodynamic flow and the electro-osmotic flow (EOF), GFP molecules can be continuously injected into the sample loading channel and stacked. We have also demonstrated that BSA is a very effective pseudo-stationary phase for sweeping concentration of proteins in comparison to the commonly used micelles. The combination of FASI and BSA sweeping yields a concentration factor of 3570 and a limit of detection of 8.4 pM for GFP. Using this method, we have separated GFP and GFP-insulin-like growth factor-I (GFP-IGF-I) fusion protein. The entire assay (GFP concentration, matrix elimination, and electrophoretic separation) can be completed within <5 min. Furthermore, we have successfully applied this method for the detection of GFP expression of *E. coli* cells and the GFP content in single *E. coli* cells.

Microchip electrophoresis (μ CE) has been one of the most active research areas over the past decade.^{1,2} Electrophoresis microchips are capable of conducting rapid analysis, reducing sample consumption, and integrating and automating multiple analytical processes. However, the concentration limits of detection of μ CE are often inadequate for the measurement of proteins/peptides at low concentration levels. Because proteins/peptides cannot be amplified as DNA via polymerase chain reaction, efficient sample preconcentration methods are highly desired for the analysis of low-abundance proteins.

Field-amplified stacking is one of the effective concentration methods, which was first discussed by Mikkers et al.³ in free-standing capillaries. Sample stacking occurs at the boundary between a high-electric-field sample zone and a low-electric-field background solution zone. A modified version of this method is a field-amplified sample injection (FASI)^{4–6} approach, which stacks the sample more efficiently. In FASI for anion analytes, the field-amplified stacking with reversed voltage control and electrokinetic sample injection happen simultaneously, resulting in more analytes being injected and concentrated at the capillary inlet.^{7–9} During stacking, the electro-osmotic flow (EOF) inside the capillary will push the sample zone toward the capillary inlet, avoiding sample matrix entering the capillary. However, care must be taken to prevent the stacked analyte zone from being pushed out of the capillary. As such, dynamically or permanently coated capillaries have been used to eliminate or reverse the EOF, to give a longer injection time. Concentration factors of 2–3 orders of magnitude have been achieved in capillary systems,^{10–12} and slightly lower concentration factors have been obtained on microchip platforms.¹³ Different schemes with complicated microchip designs and operations have been proposed to enhance the concentration factors for microchips.^{14–17} For protein analysis, field-amplified stacking can improve the limit of detection con-

- (3) Mikkers, F. E. P.; Everaerts, F. M.; Verheggen, T. J. *Chromatogr.* **1979**, *169*, 1–10.
- (4) Martinez, D.; Borrull, F.; Calull, M. J. *Chromatogr., A* **1997**, *788*, 185–193.
- (5) Zhu, L.; Lee, H. K. *Anal. Chem.* **2001**, *73*, 3065–3072.
- (6) Zhu, L.; Tham, S. Y.; Yap, A. U. J.; Lee, H. K. *J. Sep. Sci.* **2002**, *25*, 328–332.
- (7) Chien, R. L.; Burgi, D. S. *J. Chromatogr.* **1991**, *559*, 141–152.
- (8) Zhang, C. X.; Thormann, W. *Anal. Chem.* **1998**, *70*, 540–548.
- (9) Zhang, C. X.; Thormann, W. *Anal. Chem.* **1996**, *68*, 2523–2532.
- (10) Dabek-Zlotorzynska, E.; Piechowski, M. *Electrophoresis* **2007**, *28*, 3526–3534.
- (11) Xu, Y.; Wang, W. L.; Li, S. F. Y. *Electrophoresis* **2007**, *28*, 1530–1539.
- (12) Chen, Y. L.; Jong, Y. J.; Wu, S. M. *J. Chromatogr., A* **2006**, *1119*, 176–182.
- (13) Gong, M. J.; Wehmeyer, K. R.; Limbach, P. A.; Arias, F.; Heineman, W. R. *Anal. Chem.* **2006**, *78*, 3730–3737.
- (14) Lichtenberg, J.; Verpoorte, E.; de Rooij, N. F. *Electrophoresis* **2001**, *22*, 258–271.
- (15) Li, J.; Wang, C.; Kelly, J. F.; Harrison, D. J.; Thibault, P. *Electrophoresis* **2000**, *21*, 198–210.
- (16) Yang, H.; Chien, R.-L. *J. Chromatogr., A* **2001**, *924*, 155–163.

* To whom correspondence should be addressed. E-mail addresses: mpzhao@pku.edu.cn, shaorong.liu@ou.edu.

(1) Bruin, G. J. M. *Electrophoresis* **2000**, *21*, 3931–3951.

(2) Auroux, P. A.; Iossifidis, D.; Reyes, D. R.; Manz, A. *Anal. Chem.* **2002**, *74*, 2637–2652.

siderably, e.g. by 30-fold for albumin.¹⁸ The slightly declined concentration factor of FASI is resulted primarily from the relatively low electrophoretic mobility of proteins.

Pressure-driven flows have been used to offset the EOF in continuous sample injection in isotachophoretic stacking^{19,20} and FASI in capillary electrophoresis. It uses an external pressure to counterbalance the EOF during sample injection, creating a slow moving or stagnant bulk flow in the capillary column and permitting a long injection time. A great sample concentration factor is thus achieved. This method has been applied for capillary zone electrophoresis/mass spectrometry detection of single-stranded and double-stranded oligonucleotides^{21,22} and monophthalates²³ with limits of detection in the range of 0.04–0.53 ng/mL. Concentration factors of 2–3 orders of magnitude were achieved. While these pressure-assisted field-amplified sample injection approaches are successfully utilized, some of the insight details are missing. In addition, the implementation of this concept to microfluidic devices leads to more intricacies for insightful understanding, because of the geometrical complexity of the microchannel network.

Analyte sweeping is a recently developed concentration technique. Analyte concentration is achieved by entrapping and accumulating the analyte in a pseudo-stationary phase as the analyte encounters it.²⁴ Chen et al.²⁵ used semihydrodynamic pumping for sample introduction, coupled with high salt stacking and sweeping chromatography for the analysis of estrogen binding on a microchip. The sensitivity was improved by factors of 200–300 and the limits of detection decreased to 1–40 nM. Various micelle solutions have been used as pseudo-stationary phases to trap charged and uncharged analytes.^{26–30} Cyclodextrins (CDs) and polymeric substances^{31,32} have also been utilized as pseudo-stationary phases to concentrate small molecules. However, few applications have been conducted to enrich large biomolecules.

For the sensitive detection of proteins, conventional capillary electrophoresis often offers limits of detection at nanomolar levels³³ with laser-induced fluorescence (LIF) detection, although

lower limits of detection have been reported.^{34,35} Limits of detection of similar scales have also been obtained on microchips.^{36–39} Gibbons et al.⁴⁰ have reported capillary isoelectric focusing in microfluidic devices for the study of protein interactions between immunoglobulin G with protein G and antisix histidine with 6× His-tagged green fluorescent protein with LIF detection. The limit of detection was 50 fmol, corresponding to 25 pg/μL (12.5 nM). To detect low-abundance proteins in biological samples, higher sensitivity is still needed. Green fluorescent protein (GFP) and its siblings are a group of highly sensitive and universal probes in monitoring activities such as gene expression, protein localization, and protein–protein interaction in living cells and organisms.⁴¹ These fluorescent proteins are also used for in vitro bioanalysis of cells and organisms by immunoassay, electrophoresis, and chromatography.

In this paper, we report a highly effective on-chip concentration method for detection of GFP and its siblings on a simple cross-channel microchip. The method combines the field-amplified concentration and analyte sweeping, and the overall concentration factor reaches a value of >3000. With this concentration method, a detection limit of 8.4 pM is achieved for GFP. The resolution in separating GFP from its fusion protein with insulin-like growth factor-I (IGF-I) is also significantly improved. Quantitative detections of GFP expression in an *E. coli* cell population and a small number of cells in a large loading sample volume of 80 μL are achieved and the GFP content in a single *E. coli* cell is assessed, which demonstrates the potential of this on-chip concentration method for detecting trace amount of proteins.

EXPERIMENTAL SECTION

Materials and Reagents. Ni-NTA agarose was purchased from Qiagen (Hilden, Germany). The bicinechonic acid (BCA) protein assay kit was obtained from Pierce (Rockford, IL). TB buffer contained 44.5 mM Tris and 44.5 mM tetraboric acid (pH 8.0) was used as a background electrolyte (BGE) for μCE. The TB buffer with 2% (w/v) BSA was used as a BGE for BSA sweeping concentration. The sample used for field-amplified concentration was prepared in a 20-fold diluted TB buffer (pH 7.5). Other materials were purchased from local suppliers at high purity. All solutions were prepared using distilled deionized water. All chemicals employed were analytical grade and commercially available.

Instrumentation. SDS-PAGE for GFP and GFP-IGF-I was conducted in an electrophoresis system (Miniprotein-3, Bio-Rad). A ZDMCI6-1 microfluidic chip detection system (Hangzhou Syltech Technology Co., Ltd.) was used for the detection. The system consists of primarily a 488-nm argon ion laser (Model 367,

- (17) Jung, B.; Bharadwaj, R.; Santiago, J. G. *Electrophoresis* **2003**, *24*, 3476–3483.
- (18) Bessonova, E. A.; Kartsova, L. A.; Shmukov, A. U. *J. Chromatogr., A* **2007**, *1150*, 332–338.
- (19) Shackman, J. G.; Ross, D. *Anal. Chem.* **2007**, *79*, 6641–6649.
- (20) Urbánek, M.; Varenne, A.; Gebauer, P.; Kriváňková, L.; Gareil, P. *Electrophoresis* **2006**, *27*, 4859–4871.
- (21) Feng, Y. L.; Zhu, J. P. *Anal. Chem.* **2006**, *78*, 6608–6613.
- (22) Feng, Y. L.; Lian, H. Z.; Zhu, J. P. *J. Chromatogr., A* **2007**, *1148*, 244–249.
- (23) Feng, Y. L.; Zhu, J. P. *Electrophoresis* **2008**, *29*, 1965–1973.
- (24) Quirino, J. P.; Terabe, S. *Science* **1998**, *282*, 465–68.
- (25) Chen, C. C.; Yen, S. F.; Makamba, H.; Li, C. W. *Anal. Chem.* **2007**, *79*, 195–201.
- (26) Palmer, J.; Burgi, D. S.; Munro, N. J.; Landers, J. P. *Anal. Chem.* **2001**, *73*, 725–731.
- (27) Palmer, J.; Burgi, D. S.; Landers, J. P. *Anal. Chem.* **2002**, *74*, 632–638.
- (28) Markuszewski, M. J.; Britz-McKibbin, P.; Terabe, S.; Matsuda, K.; Nishioka, T. *J. Chromatogr., A* **2003**, *989*, 293–301.
- (29) Sera, Y.; Matsubara, N.; Otsuka, K.; Terabe, S. *Electrophoresis* **2001**, *22*, 3509–3513.
- (30) Sueyoshi, K.; Kitagawa, F.; Otsuka, K. *Anal. Chem.* **2008**, *80*, 1255–1262.
- (31) Otsuka, K.; Matsumura, M.; Kim, J. B.; Terabe, S. *J. Pharm. Biomed. Anal.* **2003**, *30*, 1861–1867.
- (32) Shi, W.; Palmer, C. P. *J. Sep. Sci.* **2002**, *25*, 215–221.
- (33) García-Campaña, A. M.; Taverna, M.; Fabre, H. *Electrophoresis* **2007**, *28*, 208–232.

- (34) Craig, D. B.; Wong, J. C. Y.; Dovichi, N. J. *Biomed. Chromatogr.* **1997**, *11*, 205–206.
- (35) Viskari, P. J.; Colyer, C. L. *J. Chromatogr. A* **2002**, *972*, 269–276.
- (36) Wen, J. H.; Yang, X. H.; Wang, K. M.; Tan, W. H.; Zuo, X. B.; Zhang, H. *Biosens. Bioelectron.* **2008**, *23*, 1788–1792.
- (37) Roper, M. G.; Shackman, J. G.; Dahlgren, G. M.; Kennedy, R. T. *Anal. Chem.* **2003**, *75*, 4711–4717.
- (38) Greifa, D.; Galla, L.; Rosa, A.; Anselmetti, D. *J. Chromatogr., A* **2008**, *1206*, 83–88.
- (39) Xu, Y. H.; Li, J.; Wang, R. K. *Electrophoresis* **2008**, *29*, 1852–1858.
- (40) Tan, W.; Fan, Z. H.; Qiu, C. X.; Ricco, A. J.; Gibbons, I. *Electrophoresis* **2002**, *23*, 3638–3645.
- (41) Xie, X. S.; Choi, P. J.; Li, G.-W.; Lee, N. K.; Lia, G. *Annu. Rev. Biophys.* **2008**, *37*, 417–444.

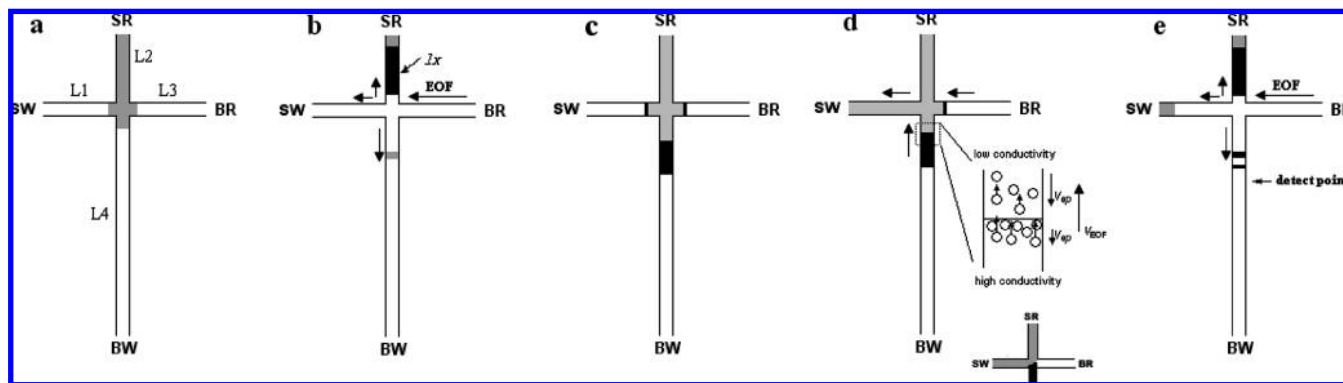


Figure 1. Schematic diagram of the sample loading, online concentrating, and separation of GFP. L₁–L₄ denotes the four parts of the microchannel. The black zone is representative of the concentrated GFP sample area. The gray zone represents the sample matrix. The arrow indicates the direction of electroosmotic flow (EOF). The inset in panel (d) depicts the distribution of sample and sample buffer at the end of step 4.

4 mW, Nanjing Electronic Equipment Corp., Nanjing, PRC) and an inverted microscope (Jiangnan Optics & Electronics Co., Nanjing, PRC). The laser beam was directed via an objective and focused to the detection point on the separation channel from below the chip. The diameter of the laser spot was 2.5 μm . The emitted light was collected by the same objective and directed to a photomultiplier tube for measurement.

Microchip Fabrication. Simple cross-channel glass microchips were kindly provided by Hangzhou Syltech Technology Co., Ltd.. The microchip was fabricated on soda–lime glass using a photolithographic and wet chemical etching process that has been described elsewhere.⁴² The channels were etched to a depth of 12 μm and a width of 48 μm . The length of the separation channel was 45 mm, and the lengths of all other channels were 5 mm to the channel intersection. Access holes were drilled into the etched plate with a 1.2-mm-diameter diamond-tipped drill bit at the terminals of the channels. After the patterned wafer was thermally bonded with a blank wafer, four micropipet tips (with an inner diameter of 4 mm and a height of 6 mm) were secured on top of the four access holes with adhesive; these assemblies served as reservoirs.

Expression and Purification of GFP and GFP-IGF-I Fusion Protein. The GFP and GFP-IGF-I expressing *E. coli* strain were obtained from our previous work by Shi et al.⁴³ Generally, *E. coli* strain BL21 (DE3) were transformed with pETGFPHis for GFP expression and pETGFP-IGFHis for GFP-IGF-I expression. The cells were grown under vigorous shaking at 37 °C in 5 mL of Luria–Bertani (LB) medium supplemented with 100 $\mu\text{g}/\text{mL}$ kanamycin. The overnight culture was inoculated in 500 mL of an LB medium containing 100 $\mu\text{g}/\text{mL}$ kanamycin under vigorous shaking at 30 °C. At $\text{OD}_{600} = 0.7$, IPTG was added to a final concentration of 0.5 mM to induce the expression of the protein, and the cells were further cultured for 6 h at 30 °C. The products were then centrifuged at 6000 rpm at 4 °C for 10 min to harvest the cells. The bacterial pellet obtained was resuspended in a lysis buffer (50 mM Na_2HPO_4 , 300 mM NaCl, 10 mM imidazole, pH 8.0) containing 1 mM phenylmethylsulfonyl fluoride (PMSF), followed by sonication. The mixture was

then centrifuged at 12 000 rpm for 30 min at 4 °C. The supernatant containing the protein was loaded onto the Ni-NTA Superflow column, which had been pre-equilibrated with the lysis buffer. The column was then washed with wash buffer (50 mM Na_2HPO_4 , 300 mM NaCl, 50 mM imidazole, pH 8.0) to remove nonspecifically bound proteins. The target protein was eluted by elution buffer (50 mM Na_2HPO_4 , 300 mM NaCl, 250 mM imidazole, pH 8.0). The eluted fractions that contained the target protein were further purified by gel filtration. The purity of the GFP and GFP-IGF-I fusion protein was determined by SDS-PAGE, using 12% (w/v) polyacrylamide MiniGels. The protein concentration was estimated using a BCA protein assay kit, and BSA was utilized as the standard.

Preparation of the Lysate of Cells. The cell suspension was collected before and after GFP expression was induced. The amount of *E. coli* cells in suspension was detected by plate count for bacterial colonies. The density of cell suspension was 1.4×10^7 colony-forming units (CFU)/mL.

For the preparation of lysate from the cell population, 1.5 mL of the original cell suspension was first centrifuged for 10 min at 6000 rpm. After the supernatant was removed, 2 mL of lyses buffer ($2 \times \text{TB}$, with 100 mM NaCl) was added. The cells were lysed by sonication for 5 min. The solution then was centrifuged for 15 min at 12 000 rpm. The supernatant was diluted 10^3 -, 10^4 -, and 10^5 -fold, respectively for on-chip electrophoresis. When the cell lysate was diluted 10^4 and 10^5 times, the samples were added to lysate buffer diluted 1000 times, to keep the electrophoresis condition constant and to prevent GFP from degradation.

For preparation of lysate from a small amount of cells, the original cell suspension was first diluted 100 times with lyses buffer, then diluted with water 1000 times, to $\sim 1.4 \times 10^2$ CFU/mL. This final cell suspension was immediately aliquoted to 100 μL per tube and lysed by sonication separately. Every aliquot was directly used for on-chip electrophoresis. It was estimated that each aliquot contained ~ 10 cells.

Chip Conditioning. The channels of a newly fabricated glass chip were washed with 98% H_2SO_4 and deionized water for 10 min each by applying a vacuum to the buffer waste reservoir (labeled as “BW” in Figure 1). The channels then were rinsed with 2.0 M NaOH for 2 h and deionized water for 10 min. Before

(42) Yin, X. F.; Shen, H.; Fang, Z. L. *Fenxi Huaxue (Chin. J. Anal. Chem.)* **2003**, 31, 116.

(43) Shi, R. N.; Huang, Y.; Wang, D.; Zhao, M. P.; Li, Y. Z. *Anal. Chim. Acta* **2006**, 578, 131–136.

every use, the channels were washed with 2.0 M NaOH, deionized water, and running buffer sequentially, for 10 min each.

μ CE Procedures. To achieve field-amplified sample stacking, the GFP sample was prepared with 20-fold diluted TB buffer. The final concentrations of GFP ranged from 2.9×10^{-8} M to 2.9×10^{-12} M. The electrophoresis running buffer was either the TB buffer or the TB buffer with 2% (w/v) BSA. The μ CE procedure can be divided into five steps:

Step 1 (Sample Preloading). Referring to Figure 1, 80 μ L of GFP sample was added to the sample reservoir (SR), while the sample waste reservoir (SW), the buffer reservoir (BR), and the buffer waste reservoir (BW) were loaded with 33.5, 33.5, and 7 μ L BGE, respectively. Because of the uneven liquid levels in the reservoirs, channel L_2 was hydrodynamically loaded with GFP sample within <8 s (see Figure 1a).

Step 2 (Field-Amplified Preconcentration). After the preloading, 2 kV was applied to BR and 1.55 kV was applied at SR and SW, while BW was grounded. This voltage setting created an overall flow (EOF plus hydrodynamic flow) from BR to all other reservoirs. Because of the conductivity difference between sample solution and BGE, GFP was electrophoretically migrating from SR to L_2 and was stacked in the BGE near the sample/BGE boundary. This concentration process required 35 s.

Step 3 (Sample Loading). After all voltages were turned off, the concentrated sample zone was allowed to hydrodynamically flow across the intersection to channel L_4 , L_2 , and L_3 (see Figure 1c). The low-conductivity sample matrix also migrated from L_2 into L_4 . This step required 30 s.

Step 4 (Reversed-Voltage Concentration). Voltages of 200, 260, and 800 V were applied at SR, BR, and BW, respectively, while reservoir SW was grounded, resulting in an overall flow to SW from all other reservoirs. As the concentrated sample zone in L_4 , which is already in the high-conductivity running buffer, moved toward the intersection, it was further concentrated and narrowed at the sample/BGE boundary, until the boundary moved to the intersection. After 10 s, the GFP zone was narrowed near the top end of L_4 , as shown in Figure 1d. The optimization of this concentration time is done by observing the EOF (sample matrix) indicator.

Step 5 (Separation). Voltages of 1.60, 1.60, and 2 kV were applied at SW, SR, and BR, respectively, and BW was grounded. The sample zone was injected into L_4 and separated, as depicted in Figure 1e.

RESULTS AND DISCUSSION

Field-Amplified Preconcentration. In our method, the sample was preloaded by hydrodynamic pressure (see Figure 1a). The preloading required 8 s for the chip that we used in this experiment. After this step, L_2 was filled with the sample, and L_1 and L_3 were mostly filled with the BGE, with small sections of them filled with sample (see Figure 1a). The loading process was fairly reproducible, as long as the relative liquid levels were kept consistent.²¹

Step 2 (field-amplified preconcentration) was executed by applying proper voltages to all reservoirs (see Figure 1b). With constant voltage supply and sample dilution ratio, the EOF velocity (V_{EOF}) and the electrophoretic velocity of the sample molecule (V_{ep}) are functions of sample plug length, whereas the hydrodynamic flow velocity (V_p) is a constant if only the relative liquid

levels in all reservoirs are maintained the same (the theoretical relationships between the sample plug length and these velocities are described in the Supporting Information).

The working principle of the field-amplified preconcentration procedure in L_2 is illustrated in Figure 2. The L_2 channel of the microchip is initially filled with a low conductivity sample solution. As Step 2 is executed, the sample solution will be pushed out toward SR by the high-conductivity BGE. Because the total voltage across L_2 will not change significantly, the field strength across the sample zone will first increase slowly at the beginning of Step 2 and then rapidly when the sample/BGE boundary approaches SR, and so does the value of V_{ep} . V_{EOF} in L_2 is an average of the electro-osmotic velocities in the sample and the BGE zones, and it is dominated by the electro-osmotic velocity of the longer zone in L_2 . Therefore, V_{EOF} decreases as the sample/BGE boundary moves toward SR, and so does the overall bulk flow velocity ($V_{2b} = V_{\text{EOF}} - V_p$). At the early stage of Step 2 (see Figures 2a and 2b), the analyte moves with the bulk flow toward SR. Because of the reduced electric field strength in the BGE zone, GFP is stacked in the BGE zone near the sample/BGE boundary. As V_{2b} decreases and V_{ep} increases, so that $|V_{2b}| < |V_{\text{ep}}|$ but in the opposite directions, the apparent velocity of analyte changes direction and the GFP molecules in the sample reservoir will migrate into L_2 and will be stacked in the BGE zone near the sample/BGE boundary (see Figure 2c). As the sample/BGE boundary continues moving toward SR, the value of V_{EOF} decreases and eventually is equal to V_p , but in the opposite directions. At this point, the bulk solution becomes stagnant while the analyte continues to migrate into L_2 (see Figure 2d). Because the bulk solution in L_2 does not move, the stacked analytes in the BGE zone will migrate slowly toward the cross region of the microchannels (see Figure 2e). A video record of the entire concentration process during Step 2 is provided in the Supporting Information. Depending on the magnitude of the hydrodynamic flow, the voltage on L_2 should be set within an appropriate range to guarantee the balance between the hydrodynamic flow and EOF. This voltage range can be estimated based on the values of V_p , L_2 , and V_{EOF} (detailed calculations are described in the Supporting Information). The viscosity differences of sample solutions will affect the value of V_p and, hence, the voltage range. In our experiment, however, the viscosity of samples is virtually a constant, because the original sample is diluted many times with a low-conductivity buffer. Under the conditions of our experiment, this range is 74–143 V.

Reversed-Voltage Concentration. After the field-amplified preconcentration, the concentrated sample was in the running buffer matrix, instead of the low-conductivity sample matrix. As all the voltages to the reservoirs were turned off, the hydrodynamic flow was resumed, bringing the concentrated sample zone across the channel intersection into L_4 . The low-conductivity sample matrix also moved into L_4 after the concentrated GFP zone. When a new set of voltages (200, 260, 800, and 0 V to SR, BR, BW, and SW, respectively) were applied, solutions in all channels flowed toward SW (see Figure 1d). Field-amplified stacking happened again, because of the presence of the boundary between the low-conductivity matrix and high-conductivity GFP-concentrated zone. GFP molecules were stacked in the running

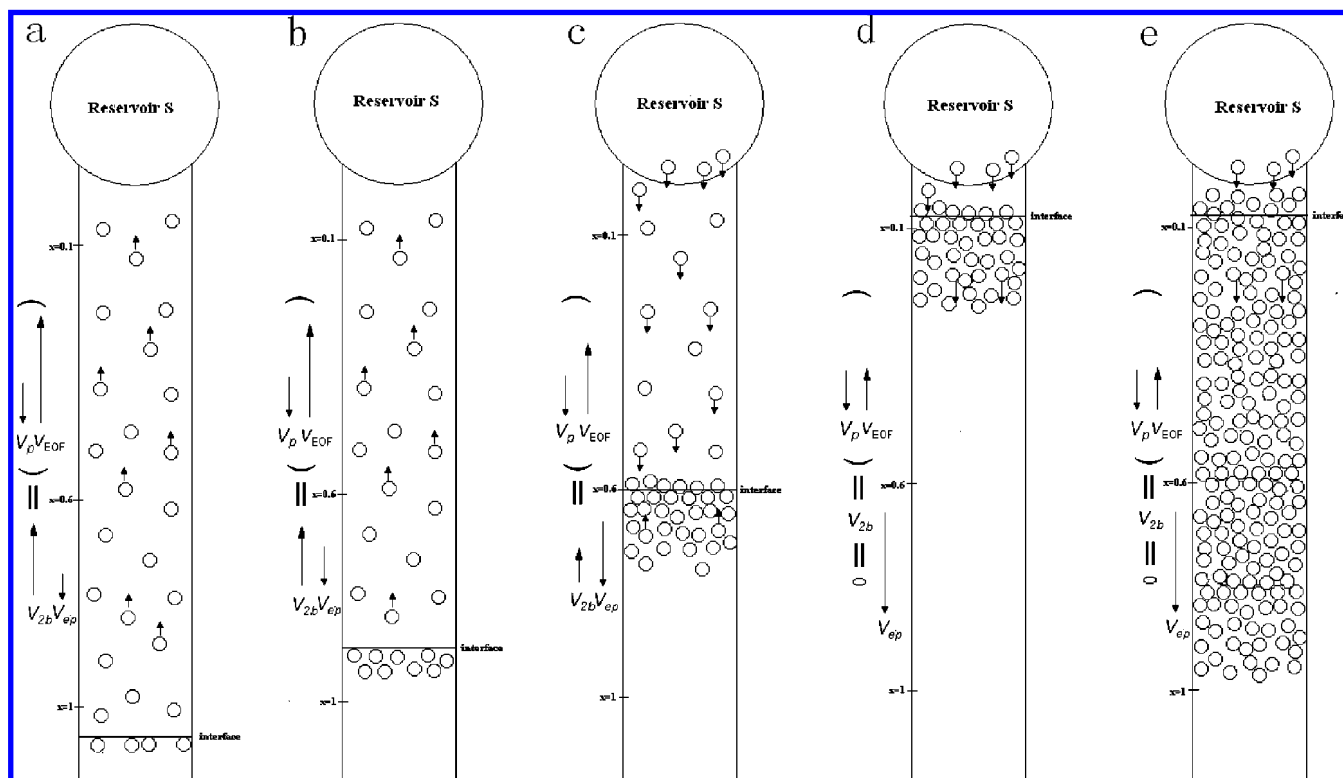


Figure 2. Schematic diagram of the field-amplified preconcentration. The circles represent for GFP molecules. First, GFP was concentrated by narrowing the existing sample zone, and then the electrophoretic velocity of GFP became greater than the bulk velocity. GFP molecules in reservoir SR moved toward the interface and accumulated. The interface then stopped moving and GFP accumulated in the entire channel of L_2 .

buffer close to the boundary. As illustrated in Figure 1c, Step 3 would inevitably bring a short plug of low-conductivity sample matrix, following a small concentrated sample zone into L_1 and L_3 . The sample plug in L_3 would be injected into L_4 in the separation mode if the reversed-voltage concentration was not performed. This would mess up the separation due to an injection of multiple sample zones. By applying the reversed voltage, the sample matrix retreated back to the intersection of L_3 and L_4 (see Figure 1d). To ensure that the GFP zone was kept in L_4 for separation as soon as it reached the top end of L_4 , we optimized the duration of the reversed-voltage concentration, using a neutral marker (Rhodamine B) as the sample and observing when Rhodamine B moved to the intersection. We selected the time for Rhodamine B to reach the intersection as the duration of the reversed-voltage concentration, which was the moment when the sharpened GFP zone following the sample matrix reached the top end of L_4 . As the voltages for Step 5 were applied, the narrow GFP zone was injected for separation, and the sample matrix was totally removed (see inset of Figure 1d). (A video record of the aforementioned process, and a corresponding explanation, have been provided in the Supporting Information.)

Both the field-amplified preconcentration and reversed-voltage concentration steps are important in achieving the highest GFP concentration factor. With the field-amplified preconcentration only, the GFP was enriched by a factor of 6 (see Figure 3, trace ii). With the reversed-voltage concentration only, GFP was concentrated by a factor of 10 (see Figure 3, trace iii). Using a combination of field-amplified preconcentration and reversed-voltage concentration, the total concentration factor was 14 (see

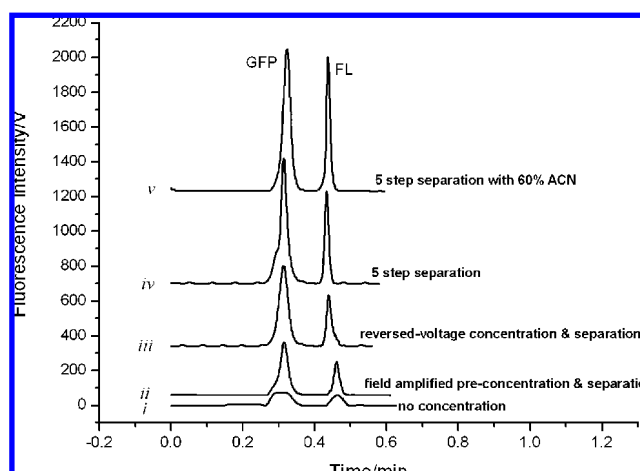


Figure 3. Signal enhancement of the field-amplified sample stacking. Trace i represents the signal intensities without any concentration. The GFP sample prepared in the running buffer was hydrodynamically introduced into the cross, followed by an electrophoretic separation. Trace ii was obtained using field-amplified preconcentration only, containing Steps a, b, c, and e. Trace iii was using reversed-voltage concentration only, containing Steps a, d, c, and e. Trace iv was obtained using a combination of field-amplified preconcentration and reversed-voltage concentration, containing all five concentration steps. Trace v was obtained in the same way as trace iv, using a sample that was prepared with a 20-fold diluted buffer in 60% acetonitrile (ACN). The sample contains 2.6×10^{-8} M GFP and 1.2×10^{-9} M fluorescein (FL).

Figure 3, trace iv). Using a sample prepared with a 20-fold diluted buffer in 60% acetonitrile (ACN), the concentration factor could be improved to 16 (see Figure 3, trace v). The concentration factor

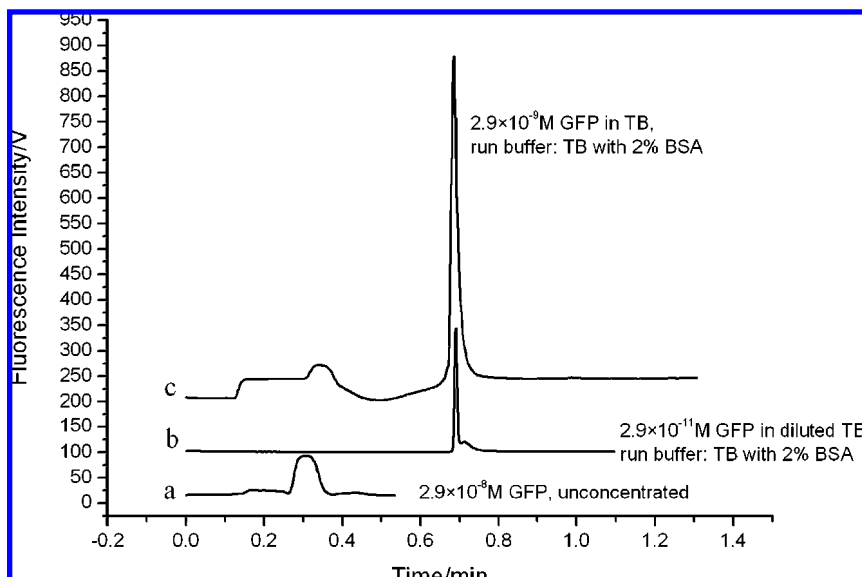


Figure 4. Signal enhancement of GFP with field-amplified concentration and BSA sweeping. The 10-fold diluted GFP sample (2.9×10^{-9} M) gives a signal that is 8.5 times higher than that by BSA sweeping. Further combining FASS with BSA sweeping gives 3570-fold concentration ratio for GFP, with a concentration of 2.9×10^{-11} M. With BSA sweeping, the impurities in GFP sample could be separated with GFP, indicating a better resolution.

was limited by the conductivity differences between the BGE and the sample solution, which is only 20 in our experiment. Apparently, higher concentration factors could be achieved with a more-diluted sample solution or a more-concentrated BGE.

Sweeping. We have tested several substances as the pseudo-stationary phases for sweeping concentration, such as sodium dodecyl sulfate (SDS), Tween 20, alanine, and polyethylene glycol (PEG). None of them showed any sweeping concentration effect in our system (data not shown). Considering that the negatively charged protein may have stronger interactions with positively charged surfactants, we also tested cetyltrimethylammonium bromide (CTAB) as the sweeping pseudo-stationary phase; still not much of an effect on sweeping concentration was obtained. In addition, because of the adsorption of CTAB on the channel surface, the charge of the channel is reversed, leading to serious adsorption of the negatively charged GFP on the channel.

Interestingly, BSA was determined to be an excellent pseudo-stationary phase for GFP sweeping. Referring to Figure 4, trace c was obtained from BSA sweeping with 2% BSA in the running buffer. Compared to trace a, which has been obtained from unconcentrated electrophoresis, BSA sweeping gives 95-fold signal enhancement. To combine the field-amplified concentration with the BSA sweeping, we used the same five-step operation procedure and experimental conditions as described in the Experimental Section for the field-amplified concentration. The only difference was to prepare the BGE in $1 \times$ TB and 2% (w/v) BSA. Referring to Figure 4, trace b was obtained with such a combined concentration approach, using a 29 pM GFP sample. The GFP peak height was more than three times higher than that of trace a, although its concentration was 1000-fold lower. A concentration factor of >3000 was yielded. The detection results for GFP were very reproducible, using the combined concentration approach, although multiple operation steps were involved. The relative standard deviations of peak height, peak area, and migration time of GFP are 5.2% and 4.9%, and 1.5%, respectively. The limit of detection, defined as $S/N = 3$, is 8.4 pM.

The mechanism of BSA sweeping currently is not very clear. To understand what BSA might have done, we have performed the following tests. First, we measured the electro-osmotic mobilities before and after the addition of BSA in the buffer. Using Rhodamine B as a neutral marker, the electro-osmotic mobilities were measured to be $6.82 \times 10^{-5} \text{ cm}^2/(\text{V s})$ in the 2% BSA buffer and $3.14 \times 10^{-4} \text{ cm}^2/(\text{V s})$ in the TB buffer. This shows that the adsorption of BSA onto the channel surface has reduced the electro-osmotic mobility. BSA adsorption prevents nonspecific adsorption of the protein analytes but could deteriorate the reproducibility of the electrophoretic separations. In our experiment, the chip was first conditioned with the running buffer before each run. For this test, the running buffer is the TB buffer with 2% BSA in it. The reproducibility results of the run-to-run (from channel washing, conditioning to the five-step concentration/separation) and the duplicate five-step concentration/separations are pretty good (see Figure S2 in the Supporting Information). These results indicated that (i) GFP adsorption was effectively prevented by the BSA additive in the buffer, and (ii) the surface modification by BSA under the experimental conditions was quite reproducible.

We have also tested the effect of different BSA concentration in the running buffer on the sweeping efficiency (see Figure 5). With 0.5% BSA in the buffer, we see only a retention time shift, caused by the adsorption of BSA on the channel surface. When the concentration of BSA is increased to 1%, the sweeping effect appears, creating a high and sharpened peak at 0.75 min. However, compared to the electropherogram obtained with 0.5% BSA, the lower peak at 0.56 min is still identifiable as the “un-swept GFP”. The sharpened peak during sweeping might be a result of the interaction between GFP and BSA. When the concentration of BSA further increases to 2%, the un-swept GFP peak disappears and the sharpened peak becomes maximized.

The separation efficiency was also improved with the addition of BSA in the running buffer. Figure 6 shows the separation results of GFP and GFP-IGF-I with and without BSA additive in the buffer.

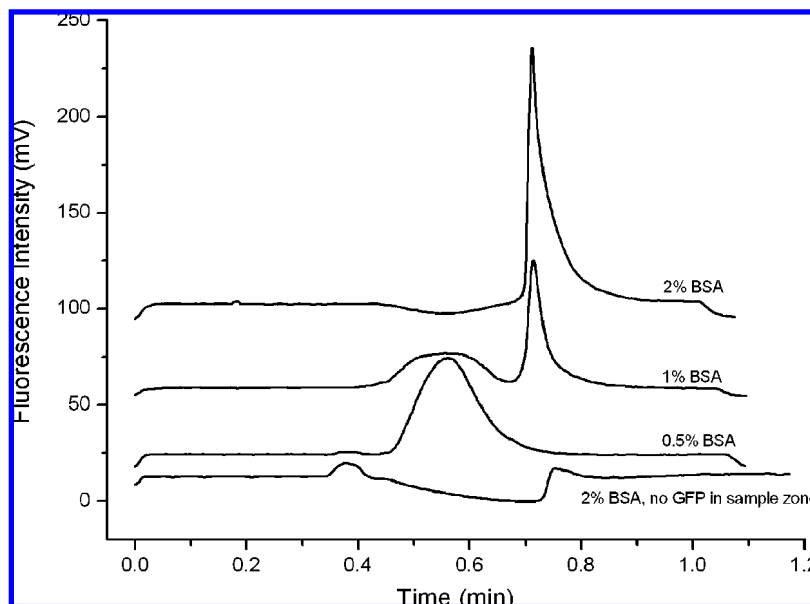


Figure 5. Comparison of the electropherograms under different BSA concentrations and the electropherogram of blank sample buffer with 2% BSA in the running buffer.

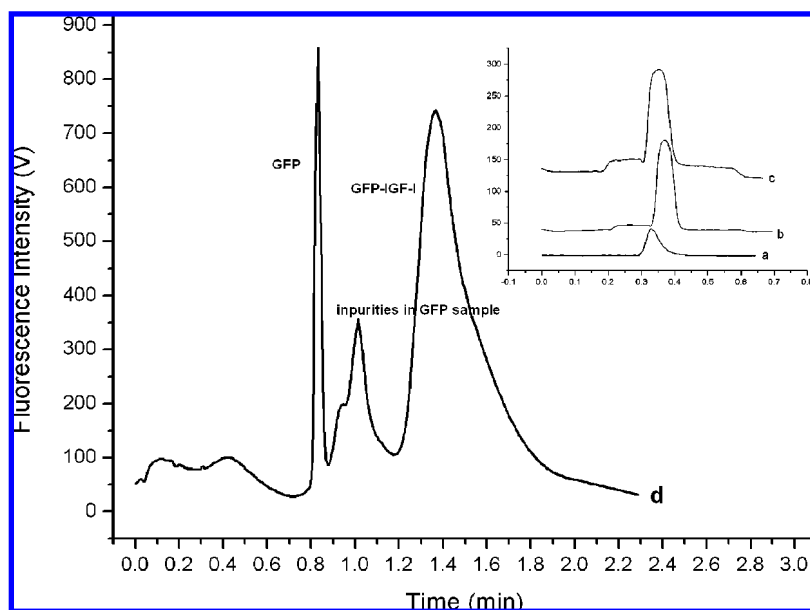


Figure 6. Traces showing the separation and concentration of GFP and GFP-IGF-I fusion protein with field-amplified sample stacking and BSA sweeping: (a) the peak of GFP under unconcentrated conditions with hydrodynamic loading and gated injection; (b) the peak of GFP-IGF-I under unconcentrated conditions; (c) the results of a mixture of GFP and GFP-IGF-I under unconcentrated conditions; and (d) the results of the same mixture of GFP and GFP-IGF-I as trace c under concentrated conditions with FASI and BSA sweeping. For the concentrated conditions, $\alpha(\text{GFP})$ is 2.9×10^{-10} M and $\alpha(\text{GFP-IGF-I})$ is 1.8×10^{-9} M. GFP and GFP-IGF-I were mixed in 20-fold diluted TB buffer (pH 7.5) and the running buffer is TB buffer containing 2% (w/v) BSA with pH 8.0. For the unconcentrated condition, $\alpha(\text{GFP})$ is 2.9×10^{-8} M and $\alpha(\text{GFP-IGF-I})$ is 5.3×10^{-8} M. Sample buffer and running buffer are both TB buffers with pH 8.0.

In the presence of BSA (see Figure 6d), GFP ($M_r = 29.4$ kD) and GFP-IGF-I ($M_r = 37.0$ kD) can be separated within <2 min. Including the sample loading and concentration, the total assay time is <5 min. Without BSA, these two proteins cannot be separated (see Figure 6c). Figure 6d also shows that the GFP-IGF-I peak is not as sharp as the GFP peak, which might be caused by a relatively weaker interaction between BSA and GFP-IGF-I than that between BSA and GFP (see more detailed discussion on this topic in the Supporting Information).

Analysis of the Lysate from the Cell Population. The calibration curve was determined by measuring standard GFP

samples at various concentrations under the same conditions as the cell lysate analysis. The standard GFP sample buffer was a 1000 \times diluted cell lyses buffer. The calibration curve shows good linearity in the range from 8.40×10^{-12} M to 1.75×10^{-9} M. The regression equation is $y = (1.11 \times 10^5)x - 2.31 \times 10^3$, where y represents the fluorescence intensity (in millivolts) and x is the concentration (given in units of 10^{-10} M). The correlation coefficient (R^2) is 0.991.

Electropherograms of lysate of *E. coli* cell population diluted 10^3 , 10^4 , and 10^5 times are shown in Figure 7a. Each sample was analyzed by consecutive electrophoresis at least five times

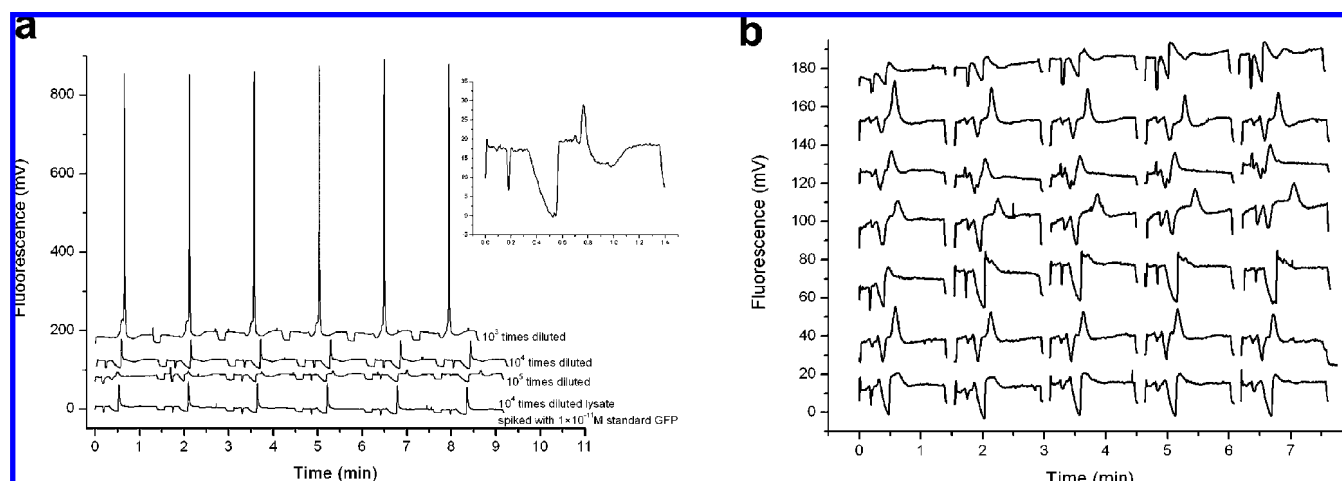


Figure 7. (a) Electropherograms of $10^3\times$ -, $10^4\times$ -, and $10^5\times$ -diluted cell content sample. The original cells were resuspended in lysis buffer ($2\times$ TB, 100 mM NaCl), lysed by sonication, centrifuged to remove cell debris, and then diluted with 1000 \times -diluted lysis buffer. The inset shows a typical electropherogram of $10^5\times$ -diluted cell content sample. (b) Electropherograms of seven samples of the content of small amount cells. Each row represents five consecutive separations of a cell content sample.

Table 1. Analytical Results of the Content of GFP in *E. coli* Cells ($n = 3$)

| dilution | fluorescence intensity (mV) | content ($\times 10^{-10}$ M) | added ($\times 10^{-10}$ M) | total ($\times 10^{-10}$ M) | recovery (%) | average amount per cell ($\times 10^{-17}$ mol) |
|--------------|-----------------------------|--------------------------------|------------------------------|------------------------------|--------------|--|
| $10^3\times$ | 564371 ± 6001 | 5.1 ± 0.1 | 3.5 | 8.2 | 95 ± 1 | 4.9 |
| $10^4\times$ | 54688 ± 384 | 0.51 ± 0.04 | 0.35 | 0.78 | 91 ± 6 | 4.9 |
| $10^5\times$ | 6256 ± 282 | 0.077 ± 0.003 | | | | 7.3 |

and each concentration was analyzed three times. The peaks were identified according to their relative migration time and the electropherograms of samples with standard GFP. To prove the reliability of the method, a certain amount of standard solutions was added to the lysate of *E. coli* cells and then measured; a typical electropherogram is shown in Figure 7a. The analyte was quantified with the concentration calibration curve. The recovery and analytical results of each diluted lysate sample are listed in Table 1. Considering the density of cell population, the average amount of GFP in individual cells can thus be estimated (see Table 1). This is the first time that GFP expression of *E. coli* cell was quantified by microchip electrophoresis. The average amount of GFP in individual cells was compared with the result from BCA protein assay, as mentioned in the Experimental Section. GFP from a 1200-mL bacterial culture with a cell density of 1.4×10^7 CFU/mL was harvested and purified, yielding 2 mL of GFP sample with a concentration of 1.74×10^{-4} M. Therefore, the estimated GFP in a single *E. coli* cell was 2.0×10^{-17} mol. Because the result was detected after the purification procedure, taking into account the loss during purification, the results from the microchip electrophoresis is reasonable.

Analysis of Lysate from a Small Number of Cells. Based on the analytical results of the lysate from the cell population, we can estimate that the $10^5\times$ diluted lysate sample represents the GFP quantity in less than 10 *E. coli* cells. Therefore, we tried to get the sample that contains ~ 10 cells to test the potential of this method for detecting proteins in single cells. Figure 7b depicts seven typical electropherograms from different aliquots of these cell samples. Because the cell number in each sample was not accurately controlled in our experiment, and because of the differences of GFP expression in single cells, the signal

intensity varies from sample to sample. With more-accurate control of the experimental parameters (e.g., the number of cells in each sample aliquot), the measurement reproducibility is expected to improve.

CONCLUSION

We have developed a method for microchip analysis of green fluorescent proteins (GFPs) at picomolar levels. The method employs a simple cross-channel glass microchip without any wall coatings and provides a novel concentration approach that combined field-amplified sample injection (FASI) and bovine serum albumin (BSA) sweeping. It is capable of concentrating GFP with a concentration factor of >3000 . This approach uses a hydrodynamic pressure from the sample reservoir in which the liquid level is relatively higher than those in other reservoirs. This pressure has been used to introduce the low-conductivity sample plug into the loading channel and counter-balance the electro-osmotic flow (EOF), so that the sample/running buffer could be kept inside the channel for prolonged field-amplified injection. Moreover, this study provides the possibility of protein concentration with sweeping method and introduces BSA as a new pseudo-stationary phase for online concentration of proteins. The addition of BSA also enables efficient separation of GFP and GFP-IGF-I fusion protein within a 1-cm-long separation channel. A proof-of-concept study of GFP expression in *E. coli* cells was demonstrated and the GFP content in single *E. coli* cell was assessed. When combined with online cell selection and lysis, this method has potential application in the detection of low-copy-number proteins in single cells. The idea of our combined concentration approach can also be extended to other applications.

ACKNOWLEDGMENT

The work was supported by the National Natural Science Foundation of China (Grant No. 90717002). S.L. was partially supported by the U.S. National Institutes of Health (No. 5 R01 GM078592-03).

SUPPORTING INFORMATION AVAILABLE

Additional information on (1) theoretical consideration of the field-amplified preconcentration and reversed-voltage concentration; (2) guidelines for voltage setting in Step 2; (3) reproducibility test results of BSA sweeping; and (4) further

investigation and discussion on the separation of GFP and GFP-IGF-I as noted in the text (PDF file). Two video records of the concentration process during Steps 2, 3, and 4 were also provided (MPG files). This material is available free of charge via the Internet at <http://pubs.acs.org>.

Received for review December 23, 2008. Accepted May 18, 2009.

AC9007607